JOURNAL OF VIROLOGY, July 2010, p. 6318–6327 Vol. 84, No. 13
0022-538X/10/$12.00 doi:10.1128/JVI.00635-10

MicroRNA miR-155 Inhibits Bone Morphogenetic Protein (BMP) Signaling and BMP-Mediated Epstein-Barr Virus Reactivation▽†

Qinyan Yin, Xia Wang, Claire Fewell, Jennifer Cameron, Hanqing Zhu, Melody Baddoo, Zhen Lin, and Erik K. Flemington*

Tulane Health Sciences Center, Department of Pathology SL79, Tulane Cancer Center, New Orleans, Louisiana 70112

Received 24 March 2010/Accepted 15 April 2010

MicroRNA miR-155 is expressed at elevated levels in human cancers including cancers of the lung, breast, colon, and a subset of lymphoid malignancies. In B cells, miR-155 is induced by the oncogenic latency gene expression program of the human herpesvirus Epstein-Barr virus (EBV). Two other oncogenic herpesviruses, Kaposi's sarcoma-associated herpesvirus and Marek's disease virus, encode functional homologues of miR-155, suggesting a role for this microRNA in the biology and pathogenesis of these viruses. Bone morphogenetic protein (BMP) signaling is involved in an array of cellular processes, including differentiation, growth inhibition, and senescence, through context-dependent interactions with multiple signaling pathways. Alteration of this pathway contributes to a number of disease states including cancer. Here, we show that miR-155 targets the 3′ untranslated region of multiple components of the BMP signaling cascade, including SMAD1, SMAD5, HIVEP2, CEBPB, RUNX2, and MYO10. Targeting of these mediators results in the inhibition of BMP2-, BMP6-, and BMP7-induced ID3 expression as well as BMP-mediated EBV reactivation in the EBV-positive B-cell line, Mutu I. Further, miR-155 inhibits SMAD1 and SMAD5 expression in the lung epithelial cell line A549, it inhibits BMP-mediated induction of the cyclin-dependent kinase inhibitor p21, and it reverses BMP-mediated cell growth inhibition. These results suggest a role for miR-155 in controlling BMP-mediated cellular processes, in regulating BMP-induced EBV reactivation, and in the inhibition of antitumor effects of BMP signaling in normal and virus-infected cells.

Despite the limited genetic content of microRNAs, their pervasive role in controlling normal and pathology-associated cellular processes has become firmly established in recent years. The importance of microRNA dysregulation in cancer is well appreciated, and a number of oncomirs and tumor suppressor microRNAs have been identified (15). As a member of the oncomir class of microRNAs, miR-155 is implicated in lymphomagenesis and a wide array of nonlymphoid tumors including breast, colon, and lung (7, 16, 24, 39, 42, 43). Despite strong evidence implicating miR-155 in cancer etiology, the mechanisms through which miR-155 supports the tumor phenotype are unclear, possibly due to limited knowledge of how predicted targets may be involved in the phenotypic properties of cancer. On the other hand, miR-155's roles in normal immune cell development and the adaptive immune response are much better understood (33, 41). These studies have demonstrated a critical role for miR-155 in immune cell activation and maturation. This evidence and other work (8, 40) have identified critical miR-155 targets whose downregulation is required for these processes.

The Epstein-Barr virus (EBV) is a human DNA tumor virus that contributes to lymphoid and epithelial cell malignancies. As a herpesvirus, a unique aspect of the EBV infection cycle is the ability to exist in either a lytic replicative state or in a latent state in which no virus is produced. Depending in part on cell background, EBV utilizes multiple forms of latency gene expression programs. True latency and type I latency are defined by the expression of no protein coding genes or by expression of the episomal replication factor EBNA1 only. Type II latency is defined by the expression of EBNA1 and the latent membrane proteins, LMP1 and/or LMP2, and is the predominant form observed in epithelial tissues. Type III latency refers to expression of the full repertoire of latency genes, which are highly tumorigenic and are capable of growth-transforming naïve resting B cells. While this form of latency is not well tolerated in immunocompetent individuals except during early stages of infection (prior to the development of adaptive immunity to these proteins), type III latency-associated lymphoid malignancies are common in immunocompromised individuals. Expression of type III latency genes in B cells mimics antigen-dependent B-cell activation, and accompanying this activation is a substantial induction of miR-155 expression (17, 20, 23, 29, 44). While it is reasonable to assume that induction of miR-155 by the type III latency program plays a role in EBV-mediated B-cell activation and oncogenesis, little is known regarding the role of miR-155 in the virus life cycle or its tumor-promoting activities.

Originally identified as cytokines critically involved in the regulation of osteogenic differentiation, bone morphogenetic proteins (BMPs) are now appreciated as having critical functions in a vast number of developmental processes. Dysregulation of BMP signaling is also implicated in disease states including cancer (1). The canonical signaling pathway stimulated by BMP receptor engagement is the phosphorylation of the SMADs (mothers against decapentaplegic homologs), SMAD1, SMAD5, and SMAD9, which facilitates

* Corresponding author. Mailing address: Tulane Health Sciences Center, SL79, 1430 Tulane Avenue, New Orleans, LA 70112. Phone: (504) 988-1167. Fax: (504) 988-5516. E-mail: eflemin@tulane.edu.

† Supplemental material for this article may be found at http://jvi.asm.org/.

▽ Published ahead of print on 28 April 2010.

active transport of these mediators from the cytoplasm to the nucleus, where they bind and activate cellular promoters. While these signaling mediators are considered to have fairly redundant activities, the influence of BMP activation can have widely distinct outcomes on a particular cell depending on cellular context (3, 27). These distinctions arise from the innate low-affinity DNA binding properties of SMADs and the concordant requirement for any of a broad range of cofactors that facilitate high-affinity binding to specific sets of promoters. Using this signaling mechanism, the phenotypic outcome of BMP receptor engagement is controlled by the level of activation of other signaling pathways and SMAD binding cofactors. While activation of BMP signaling appears to contribute to some cancer types, it inhibits other cancer types by promoting growth arrest and differentiation and by inducing senescence (1). In immune cells, BMP signaling has been shown by multiple groups to inhibit lymphocyte activation, maturation, and growth (2, 6, 13, 18, 19, 37). Here, we show that miR-155 inhibits BMP signaling by targeting multiple factors in the BMP signal transduction cascade. This function may be important during immune cell activation by preventing BMP from impeding this process, it may be important for the survival of EBV type III latency associated tumors by preventing BMP-mediated viral reactivation and cell death, and it may be relevant to other cancer types by blocking growth arrest properties of BMPs.

MATERIALS AND METHODS

Cell culture. Mutu I and A549 cells were maintained in RPMI 1640 medium and Dulbecco's modified Eagle's medium (DMEM), respectively, supplemented with 10% fetal bovine serum (FBS) plus 0.5% penicillin-streptomycin. All cells were maintained at 37°C with 5% CO_2 in a tissue culture incubator.

Plasmid construction. Generation of the pMSCV-puro-GFP-miR-CNTL (where GFP is green fluorescent protein) and pMSCV-puro-GFP-miR-155 retroviral expression vectors was previously described (44). The 3′ untranslated region (UTR) reporter plasmids were generated by PCR amplification of the relevant 3′ UTR regions from genomic DNA, and the fragments were cloned into the reporter vector pMIR-REPORT-dCMV (44). The 3′ UTR coordinates (based on the TargetScan database [22]) cloned for each gene are as follows: CEBPB, 421 to 604, HIVEP2, 548 to 1752; MYO10, 430 to 842; RUNX2, 798 to 3569; SMAD1, 288 to 907; and SMAD5, 12 to 928. For analysis of SMAD1 and SMAD5 miR-155 and miR-17 3′ UTR mutant analysis, wild-type or mutant versions of 3′ UTR sequences spanning either 288 to 437 (SMAD1) or 685 to 905 (SMAD5) were synthesized by BlueHeron Biotechnology and cloned into pMIR-REPORT-dCMV.

3′ UTR-luciferase reporter analysis. A total of 3.75 μg of either the control (pMSCV-puro-GFP-miR-CNTL) or miR-155 (pMSCV-puro-GFP-miR-155) expression vector was cotransfected with 0.25 μg of the appropriate pMIR-REPORT-dCMV 3′ UTR reporter plasmid into 1×10^6 Mutu I cells using Lipofectamine (Invitrogen). Cells were harvested at 48 h posttransfection and analyzed using a Promega luciferase assay. Values reported are expression change of a given 3′ UTR relative to change in the control reporter.

Real-time RT-PCR analysis of cellular mRNA levels. Total RNA was prepared using an miRNeasy kit (Qiagen), and cDNA was synthesized using a SuperScript III First-Strand Synthesis System (Invitrogen). Real-time PCR was conducted using an iQ5 multicolor real-time PCR detection system (Bio-Rad) with the following conditions: 95°C for 3 min followed by 40 cycles of 95°C for 30 s, 62°C for 40 s, and 72°C for 40 s. Reverse transcription-PCR (RT-PCR) primers are listed in Table S1 in the supplemental material. Mature miR-155 real-time RT-PCR was carried out at 95°C for 3 min, followed by 40 cycles of 95°C for 15 s and 60°C for 30 s.

Western blot analysis. Cells were lysed by suspension in 1× SDS-PAGE loading buffer and heated at 95°C for 20 min to shear genomic DNA. Protein concentrations were determined using an ND-1000 spectrophotometer (NanoDrop). Twenty-five micrograms of total protein was loaded in each well, separated on a 4 to 20% Tris-HCl Criterion Precast gel, and transferred to a nitrocellulose transfer membrane. The membranes were incubated overnight at 4°C with primary antibody (See Table S2 in the supplemental material) in Tris-buffered saline (TBS) containing 5% low-fat powdered milk; the membranes were washed three times (10 min each) in TBS buffer and incubated for 1 h at room temperature with the appropriate secondary antibody (See Table S2) in TBS buffer containing 5% low-fat powdered milk. Membranes were washed three times (10 min each) in TBS buffer and subjected to image analysis using an Odyssey infrared imaging system (Li-Cor).

Generation of stable miR-155-expressing cell lines. Retrovirus preparations were generated through transient cotransfection of 293 cells with retroviral expression vectors plus packaging vectors. Transient transfections were performed using a modified version of the calcium phosphate precipitation procedure. Briefly, 10^6 HEK293 cells were plated onto 100-mm-diameter tissue culture dishes. The following day, the medium was replaced with 8 ml of fresh supplemented DMEM. Four hours later, DNA precipitates were generated by mixing 0.5 ml of 1× HEPES-buffered saline (0.5% HEPES, 0.8% NaCl, 0.1% dextrose, 0.01% anhydrous Na_2HPO_4, 0.37% KCl [pH 7.10]) with a total of 30 μg of plasmid DNA (10 μg of retroviral vector, 10 μg of vesicular stomatitis virus G protein expression vector, and 10 μg of pVPACK dGI packaging vector). Thirty microliters of 2.5 M $CaCl_2$ was added, and samples were mixed immediately after each addition. Precipitates were allowed to form at room temperature for 20 min before being added in a dropwise fashion to cells. Cells were incubated at 37°C with 5% CO_2 for 16 h before the medium was replaced with 10 ml of fresh DMEM (plus 10% FBS).

Forty-eight hours later, viral supernatants were collected and subjected to one round of centrifugation, followed by filtration through a 0.45-μm-pore-size surfactant-free cellulose acetate filter. Infections were carried out in six-well plates with 1 ml of virus plus 4×10^6 Mutu I cells (suspended in 1 ml of complete RPMI medium plus 24 μg/ml Polybrene) or 1×10^5 A549 cells (in 1 ml of complete DMEM plus 24 μg/ml Polybrene) per well. Cells were spun in six-well plates at $1{,}000 \times g$ for 1 h at room temperature, followed by a 4-h incubation at 37°C with 5% CO_2. Medium was then removed from A549 infections and replaced with fresh complete DMEM. Mutu I cells were collected, spun down, and resuspended in 4 ml of complete RPMI medium per well. Cells were cultured for 2 days prior to selection with 1 μg/ml puromycin and were analyzed after 10 to 14 days of puromycin selection.

BMP treatment. BMP6 was purchased from R&D Systems, and BMP2 and BMP7 were purchased from Miltenyi Biotec. For treatment of Mutu I and Mutu III cells, 2×10^6 cells were spun down, resuspended in 2 ml of complete medium, and seeded on each well of a six-well plate. Two hours later, BMPs were added to a final concentration of 1 μg/ml. For treatment of A549 cells, 3×10^5 cells were plated in each well of a six-well plate containing 2 ml of complete medium. Two days later, medium was changed and replaced with DMEM containing 1% FBS in the morning. Following 8 h of incubation at 37°C with 5% CO_2, BMPs were added to a final concentration of 1 μg/ml. Cells were harvested at the times indicated in the figure legends.

Quantitative analysis of viral genomes in culture medium. Forty-eight hours after exposure of Mutu I cells to the indicated BMPs, cells were spun down, and the medium was filtered through a 0.45-μm-pore-size surfactant-free cellulose acetate filter. Proteinase K was added to the medium to a final concentration of 1 mg/ml and incubated at 37°C for 1 h, followed by incubation at 95°C for 10 min. The medium was then subjected to phenol-chloroform extraction and diluted 10-fold in H_2O. Two microliters of each diluted sample was used for real-time PCR analysis of viral DNA, and PCRs were carried out using two different sets of primers (sequences are listed in Table S1 in the supplemental material) designed to amplify a region of either the BamHI Z locus or the BamHI Q locus. Real-time PCR was conducted using an iQ5 PCR machine with the following conditions: 95°C for 3 min followed by 40 cycles of 95°C for 30 s, 62°C for 40 s, and 72°C for 40 s using Eva green Supermix (Bio-Rad).

A549 cell growth analysis. For colony formation assay, 500 control- or miR-155-expressing A549 cells were seeded into each well of a six-well plate. Cells were cultured in 1% FBS medium with or without BMP2 for 14 days prior to analysis of cell colony formation. Colonies were stained with crystal violet blue and analyzed using a Colcount Cell Counter (Oxford Optronix).

RESULTS

miR-155 targets members of the BMP signaling pathway. In a previous report investigating the interplay between miR-155 and Epstein-Barr virus infection, we had shown that the 3′ UTR of SMAD5 can be inhibited by miR-155 in a 3′ UTR

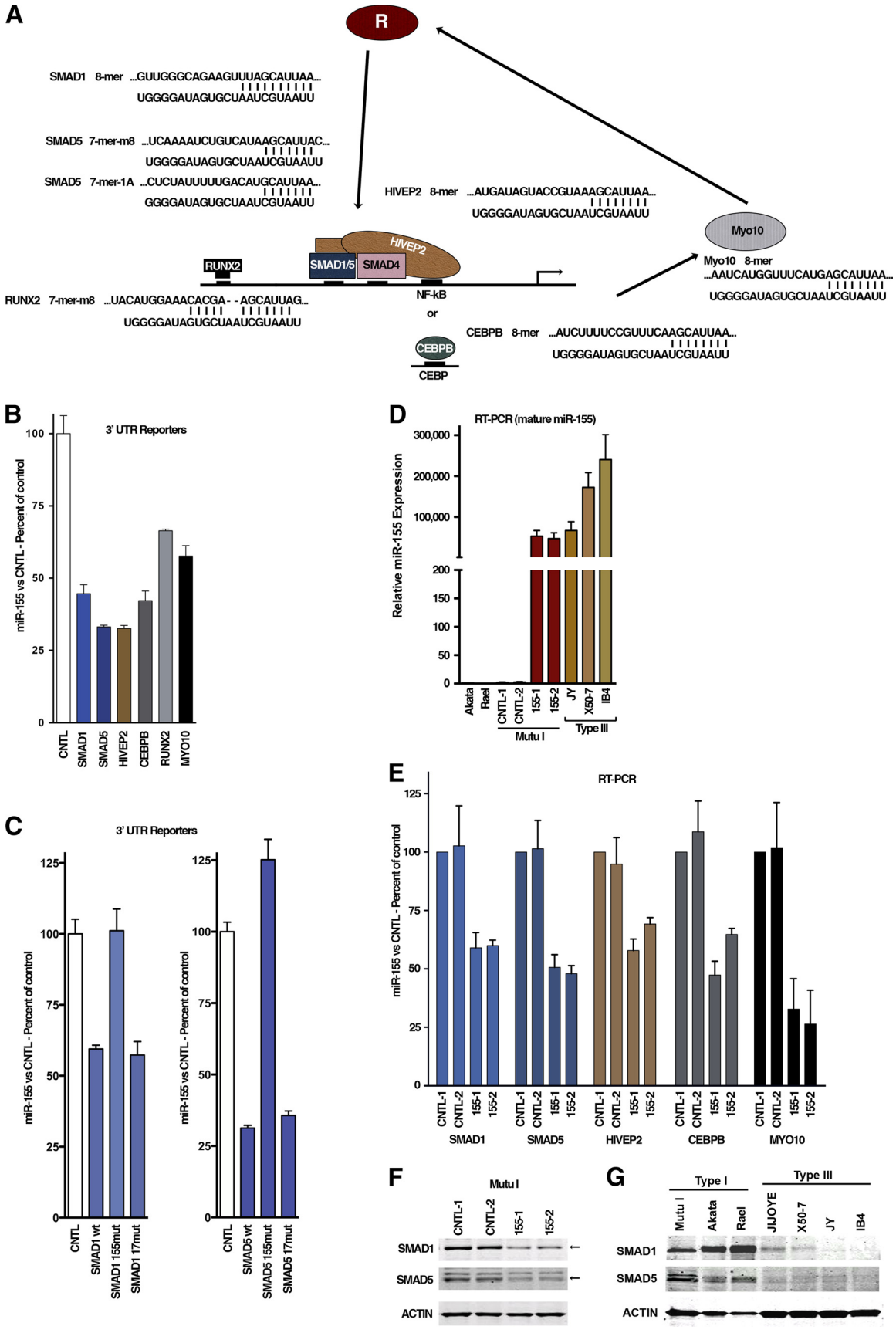
A
R
SMAD1 8-mer ...GUUGGGCAGAAGUUUAGCAUUAA...
UGGGGAUAGUGCUAAUCGUAAUU
SMAD5 7-mer-m8 ...UCAAAAUCUGUCAUAAGCAUUAC...
UGGGGAUAGUGCUAAUCGUAAUU
SMAD5 7-mer-1A ...CUCUAUUUUUGACAUGCAUUAA...
GGGGAUAGUGCUAAUCGUAAUU
HIVEP2 8-mer ...AUGAUAGUACCGUAAAGCAUUAA...
UGGGGAUAGUGCUAAUCGUAAUU
Myo10
Myo10 8-mer
...AAUCAUGGUUUCAUGAGCAUUAA...
UGGGGAUAGUGCUAAUCGUAAUU
HIVEP2
SMAD1/5
SMAD4
RUNX2
NF-kB
or
CEBPB
CEBP
RUNX2 7-mer-m8 ...UACAUGGAAACACGA- - AGCAUUAG...
UGGGGAUAGUGCUAAUCGUAAUU
CEBPB 8-mer ...AUCUUUUCCGUUUCAAGCAUUAA...
UGGGGAUAGUGCUAAUCGUAAUU
B
3' UTR Reporters
miR-155 vs CNTL - Percent of control
CNTL
SMAD1
SMAD5
HIVEP2
CEBPB
RUNX2
MYO10
C
3' UTR Reporters
miR-155 vs CNTL - Percent of control
CNTL
SMAD1 wt
SMAD1 155mut
SMAD1 17mut
SMAD5 wt
SMAD5 155mut
SMAD5 17mut
D
RT-PCR (mature miR-155)
Relative miR-155 Expression
Akata
Rael
CNTL-1
CNTL-2
155-1
155-2
JY
X50-7
IB4
Mutu I
Type III
E
RT-PCR
miR-155 vs CNTL - Percent of control
SMAD1
SMAD5
HIVEP2
CEBPB
MYO10
F
Mutu I
SMAD1
SMAD5
ACTIN
G
Type I
Type III
Mutu I
Akata
Rael
JIJOYE
X50-7
JY
IB4
SMAD1
SMAD5
ACTIN

reporter experiment (44). This suggested that miR-155 may target endogenous SMAD5 transcripts and that it may disrupt BMP signaling. Nevertheless, we had not shown that inhibition of the 3′ UTR was mediated through the predicted miR-155 target sites, and we had not investigated whether the endogenous gene was affected by miR-155.

MicroRNAs frequently target multiple members of signaling pathways, possibly as a means to exert stronger influences on the respective pathway in the face of their typically moderate inhibitory effects on individual genes. An informatics analysis of the complete list of 3′ UTRs (from the TargetScan 3′ UTR database [22]) containing conserved or nonconserved miR-155 seed sequences of at least 7-mer revealed a number of potential miR-155 target genes in the BMP signaling pathway in addition to SMAD5 (Fig. 1A). The 3′ UTR of another BMP-responsive SMAD, SMAD1, was also found to have a predicted 8-mer target site. Cofactors involved in facilitating promoter binding specificity of SMAD1 and SMAD5 were also found to have predicted miR-155 target sites in their 3′ UTRs, including RUNX2, HIVEP2 (Schnurri-2), and CEBPB (Fig. 1A). Lastly, a downstream target of BMP signaling, MYO10, which has been shown previously (30) to be involved in an autoactivation loop, was found to contain a predicted 8-mer miR-155 target site (Fig. 1A).

To assess targeting of these 3′ UTRs by miR-155, 3′ UTR reporters for each of these BMP signaling intermediates were cotransfected into the EBV-positive Burkitt's lymphoma cell line Mutu I with either a control expression vector (pMSCV-puro-GFP-miR-CNTL) or an miR-155 expression vector (pMSCV-puro-GFP-miR-155). Although the level of inhibition varied, the 3′ UTRs of each of these genes were found to be inhibited by miR-155 (Fig. 1B). Since SMAD1 and SMAD5 are critical transducers of cytoplasmic to nuclear BMP signaling, we further investigated the specificity of SMAD1 and SMAD5 targeting. Mutant versions of the SMAD1 and SMAD5 3′ UTR reporters were generated in which the single miR-155 binding site in SMAD1 and the two miR-155 binding sites in SMAD5 were mutated. We also noted that there are proximal predicted target sites for another oncogenic family of microRNAs, the miR-17 cluster microRNAs, with close proximity to the miR-155 target sites in both the SMAD1 and the SMAD5 3′ UTRs. We had shown previously that members of the miR-17 family are expressed in Mutu I cells (5), so we also generated separate mutants of the miR-17 sites in these reporters to determine whether there might be proximity-based synergy between miR-155 and miR-17 microRNAs. Mutation of the miR-155 target sites in SMAD1 or SMAD5 resulted in a loss of miR-155 repression (Fig. 1C). Therefore, miR-155 targets SMAD1 and SMAD5 through binding to their respective predicted miR-155 target sites in their 3′ UTRs. Mutation of the miR-17 family binding sites in either SMAD1 or SMAD5 did not influence the ability of miR-155 to inhibit expression of these reporters, indicating that there is no apparent dependency on proximity-based synergy with miR-17 family microRNAs (Fig. 1C).

miR-155 inhibits the expression of endogenous SMAD1 and SMAD5. To assess the ability of miR-155 to influence endogenous SMAD1 and SMAD5 gene expression, the type I latency cells, Mutu I, were transduced with either a control (pMSCV-puro-GFP-miR-CNTL)- or a miR-155 (pMSCV-puro-GFP-miR-155)-expressing retrovirus. Duplicate control and duplicate miR-155 retroviral transductions were carried out to help rule out the possibility that observable changes are due to culturing-associated gene expression drifting. In each case, approximately 4×10^6 cells were infected, and infection rates were judged to be greater than 50%, based on the number of GFP-expressing cells 2 days following infection. RNA and protein extracts were prepared from infected cells 10 days after selection. miR-155-transduced Mutu I cells were found to express miR-155 at levels comparable to the endogenous levels observed in EBV-infected B cells exhibiting type III latency (Fig. 1D).

To determine whether endogenous SMAD1, SMAD5, HIVEP2, CEBPB, or MYO10 genes are regulated by miR-155, quantitative RT-PCR analysis was carried out in retrovirally transduced Mutu I cells (note that RUNX2 is not expressed in these cells since it could not be detected by RT-PCR analysis or by next-generation sequencing [G. Xu, C. Fewell, C. Taylor, N. Deng, D. Hedges, X. Wang, K. Zhang, M Lacey, H. Zhang, Q. Yin, J. Cameron, Z. Lin, D. Zhu, and E. K. Flemington, submitted for publication]). Expression levels of SMAD1, SMAD5, HIVEP2, CEBPB, and MYO10 were found to be lower in cells transduced with the miR-155 retrovirus (Fig. 1E). Further, SMAD1 and SMAD5 protein levels were lower in miR-155-transduced Mutu I cells (Fig. 1F). Lastly, we assessed the levels of SMAD1 and SMAD5 in EBV-positive B-cell lines displaying either type I (low miR-155) or type III (high miR-155) latency. SMAD1 and SMAD5 expression was lower in EBV-infected B cell lines displaying type III latency than in three EBV-infected B-cell lines displaying type I latency (Fig. 1G). Together, these data show that miR-155 targets multiple factors of the BMP signaling pathway in EBV-infected B cells.

FIG. 1. miR-155 inhibits members of the BMP signaling pathway. (A) Schematic of BMP signaling genes with potential miR-155 target sites. R, BMP receptor. (B) 3′ UTR reporter analysis of predicted miR-155 targets was performed in Mutu I cells. (C) Analysis of wild-type SMAD1 and SMAD5 3′ UTR reporters and corresponding reporters with either the miR-155 (155mut) or miR-17 (17mut) target sites mutated was carried out in Mutu I cells. (D) Expression of mature miR-155 was analyzed by real time RT-PCR in Mutu I cells transduced with a control (CNTL-1 and CNTL-2)- or a miR-155 (155-1 and 155-2)-expressing retrovirus and the EBV-positive type I (Akata and Rael) and type III (JY, X50-7, and IB4) latency cells. Real-time RT-PCR was performed using a mirVana microRNA detection kit (Ambion) with a mirVana quantitative RT-PCR miR-155 primer set and a 5S primer set (Ambion). Relative miR-155 expression was calculated using the $2^{-\Delta\Delta Ct}$ method (C_T is threshold cycle), where $\Delta\Delta C_T = (\Delta C_T$ average in the type I cells$) - (\Delta C_T$ in each cell line) (the type I cells are Akata and Rael), and $\Delta C_T = (C_T$ value of miR-155$) - (C_T$ value of 5S RNA). (E) Real-time RT-PCR analysis of miR-155 targets in retrovirally transduced control and miR-155 Mutu I cells. Values reported are the percent expression relative to CNTL-1 $2^{-\Delta\Delta Ct}$. C_T values were normalized to glyceraldehyde-3-phosphate dehydrogenase C_T values obtained from the same cDNA samples. (F) Western blot analysis of SMAD1 and SMAD5 (Sigma) protein levels in control- or miR-155-transduced Mutu I cells. (G) SMAD1 and SMAD5 (Sigma) protein expression was analyzed in the EBV-infected type I (Mutu I, Akata, and Rael) and type III (JIJOYE, X50-7, JY, and IB4) cell lines by Western blot analysis.

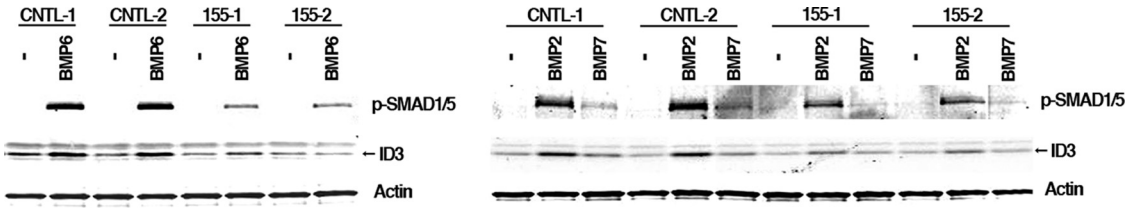

FIG. 2. miR-155 inhibits BMP2-, BMP6-, and BMP7-mediated induction of ID3. Retrovirally transduced control (CNTL-1 and CNTL-2) or miR-155 (155-1 and 155-2) Mutu I cells were treated with the indicated BMP and harvested 48 h later for Western blot analysis. −, no treatment.

miR-155 inhibits BMP-mediated induction of ID3. Having determined that miR-155 can inhibit the expression of BMP signaling intermediates, we next assessed whether this suppression influenced the ability of BMP to signal to downstream targets. Mutu I cells were found to be responsive to BMP2, BMP6, and BMP7, as evidenced by the induction of phospho-SMAD1/SMAD5 (SMAD1/5) in control-transduced Mutu I cells (Fig. 2) although the degree of phospho-SMAD1/5 induction by BMP7 was less robust (at this 48-h time point) than that observed for BMP2 and BMP6. In line with expectations, miR-155-transduced Mutu I cells showed lower levels of phosphorylated SMAD1/5 (Fig. 2) in response to BMP2, -6, and -7. Inhibitor of differentiation (ID) proteins are canonical downstream targets of BMP signaling. In repeated attempts, we could not detect the ID1 or ID2 family members before or after exposure to BMPs by Western blot analysis in Mutu I cells. In contrast, ID3 was detected and was increased in response to BMP2, -6, and -7 (Fig. 2). Moreover, ID3 induction was dampened in miR-155-transduced cells. This indicates that miR-155-mediated inhibition of BMP signaling intermediates negatively influences the ability of BMP to induce downstream targets.

BMP2, BMP-6, and BMP-7 induce Epstein-Barr virus reactivation. Previous studies have shown that transforming growth factor β (TGF-β) can induce reactivation in EBV-infected B cells exhibiting type I latency (35). This raised the possibility that BMP signaling may similarly induce EBV reactivation in type I latency cells and that miR-155 expression may suppress BMP-induced reactivation. Despite similarities in the TGF-β and the BMP signaling pathways, induction of gene expression by these two classes of mediators is facilitated through the cooperation with a number of distinct pathway-specific cofactors, and in some settings, these pathways have been shown to interfere with each other. To our knowledge, no previous studies have tested whether BMP proteins can induce EBV reactivation. To assess this possibility, Mutu I cells were exposed to BMP6, TGF-β, BMP6 plus TGF-β, BMP2, or BMP7. Cells were collected for Western blot analysis, and medium was collected for detection of viral DNA (reflective of the level of secreted viral particles). As expected, BMP2, -6, and -7 induced phospho-SMAD1/5 while TGF-β induced the level of phospho-SMAD2 (Fig. 3A and B). Consistent with previous studies, TGF-β induced the expression of the immediate-early and early Zta, Rta, and BMRF1 viral genes (Fig. 3A), as well as the production of secreted virus (Fig. 3C). BMP6 was found to induce Zta, Rta, and BMRF1 expression and virus production, but the levels of induction were modest compared to the level of induction observed with TGF-β (Fig. 3A). Addition of

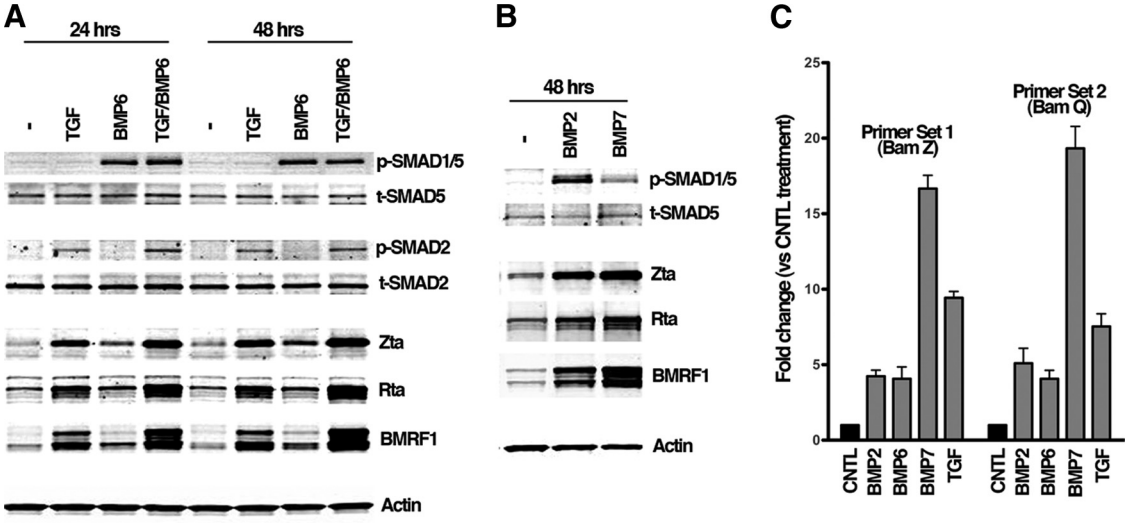

FIG. 3. BMP signaling induces EBV reactivation. Mutu I cells were exposed to BMP2, BMP6, BMP7, and/or TGF-β for the indicated times, and cells were collected for Western blot analysis (A and B). Antibodies used are listed in Table S2 in the supplemental material (the SMAD5 antibody used here is from Cell Signaling). (C) Medium was collected for real-time PCR analysis of viral genomes after 48 h of treatment. Primer set 1 and set 2 were designed to amplify a portion of the BamHI Z and BamHI Q regions of the EBV genome, respectively. The relative fold change of BMP- and TGF-β-treated samples was calculated based on the C_T value of untreated (CNTL) cells. −, no treatment.

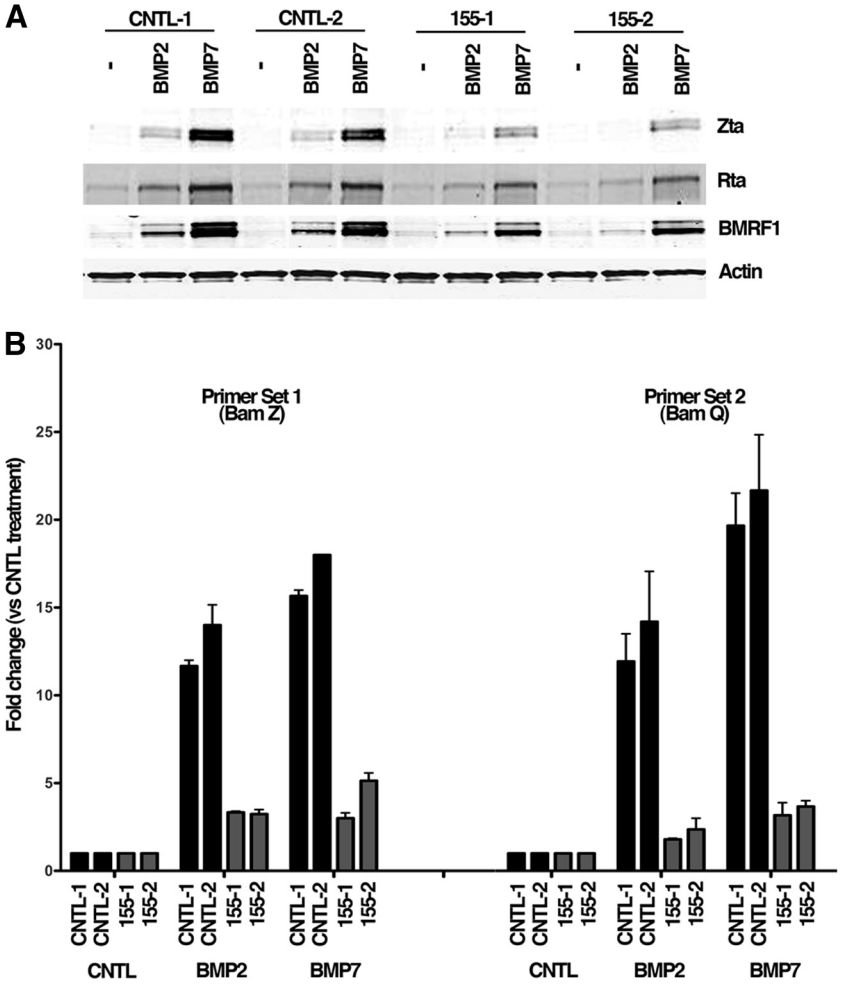

FIG. 4. miR-155 inhibits BMP-mediated EBV reactivation. (A) Western blot analysis of control, BMP2-, or BMP7-treated control (CNTL-1 and CNTL-2)- or miR-155 (155-1 and 155-2)-expressing Mutu I cells showing inhibition of EBV immediate-early and early lytic Zta, Rta, and BMRF1 genes at 48 h after treatment. Actin is a loading control. (B) Real-time PCR analysis of EBV viral DNA extracted from the medium of control and BMP2- or BMP7-treated Mutu I cultures 48 h after treatment. PCR primers (see Table S1 in the supplemental material) were designed to amplify regions of the BamHI Z or BamHI Q region of the EBV genome. The relative C_T value fold change of BMP-treated samples is calculated on the basis of the C_T value of untreated (CNTL) cells. −, no treatment.

both BMP6 and TGF-β did not result in any observable cross-interference. Instead, treatment with both of these agents had an enhanced influence on Zta, Rta, and BMRF1 expression. Exposure of Mutu I cells to BMP2 and BMP7 resulted in a more robust induction of Zta, Rta, and BMRF1 than treatment with BMP6 (Fig. 3A and B). Further, at least in the case of BMP7, the level of virus in the medium surpassed the level observed with TGF-β (Fig. 3C). Together, these results indicate that although there appear to be amplitude differences in signaling mediated by BMP2, -6, and -7, activation of the BMP pathway can facilitate EBV reactivation in Mutu I cells.

miR-155 inhibits BMP-mediated EBV reactivation. To analyze whether miR-155 influences BMP-mediated reactivation, Zta, Rta, and BMRF1 expression levels were monitored following BMP treatment of Mutu I cells transduced with control or miR-155 retroviruses. miR-155 suppressed induction of each of these lytic proteins in cells treated with BMP2 or BMP7 (Fig. 4A). Similarly, despite a lower level of reactivation induced by BMP6, suppression of Zta and Rta induction by miR-155 was also evident (see Fig. S1 in the supplemental material). Inhibition of BMP2- and BMP7-induced reactivation was also manifested in the form of marked decreases in the number of viral genomes detected in the medium (Fig. 4B). From these data we draw the conclusions that miR-155 is able to inhibit BMP signaling and that functionally relevant levels of miR-155 (similar to the levels observed in EBV-infected B cells displaying type III latency) are capable of inhibiting BMP-induced transitioning from latency to lytic reactivation. Consistent with the latter assertion, BMP2, BMP6, and BMP7 are not able to induce Zta, Rta, or BMRF1 expression in Mutu III cells (the isogenic type III latency derivative of Mutu I cells) (Fig. 5).

miR-155 inhibits BMP signaling in the lung epithelial cell line A549. To gain some insight into the generality of miR-155-mediated inhibition of BMP signaling, we extended our study to the human lung epithelial cell line A549. A549 cells were transduced in duplicate with control- or miR-155-expressing retrovirus and assayed for SMAD1 and SMAD5 expression

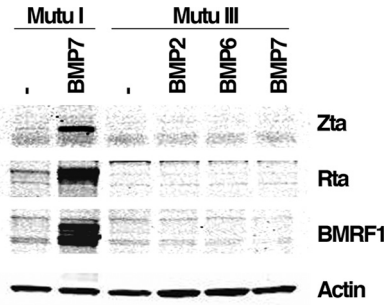

FIG. 5. Type III latency cells, Mutu III, are not responsive to BMP2, BMP6, or BMP7. Mutu I and Mutu III cells were treated as described in Materials and Methods and analyzed for Zta, Rta, and BMRF1 expression by Western blot analysis 48 h after cytokine addition.

by Western blot analysis. Similar to the results obtained in Mutu I cells, SMAD1 and SMAD5 levels were found to be lower in A549 cells expressing miR-155 (Fig. 6A).

We next treated control- or miR-155-expressing A549 cells with BMP2, -6, or -7 and generated protein extracts at 24 h posttreatment. Good induction of phospho-SMAD1/5 was observed in control cells, and the levels of phospho-SMAD1/5 were found to be reduced in miR-155-expressing cells. Previous studies have shown that BMP2 induces expression of the cyclin-dependent kinase inhibitor p21, along with a transient growth inhibition (4, 11). Consistent with these results, Western blot analysis of p21 expression in extracts from A549 cells treated with BMP2, -6, and -7 showed induced levels of p21 by each of these BMPs (Fig. 6B). In contrast, induction of p21 was largely abrogated in miR-155-expressing cells, indicating that miR-155 is capable of functionally inhibiting BMP signaling in this system.

To gain insights into the implications of the effect of miR-155 on BMP-mediated growth inhibition, control- or miR-155-transduced A549 cells were plated at a low density, treated with BMP2, and grown for 2 weeks prior to staining with crystal violet blue to determine colony growth. Fewer colonies were observed in BMP2-treated control cells than in untreated cells, whereas similar numbers of colonies were observed in BMP2-treated and untreated miR-155-expressing cells (Fig. 6C). From these data, we conclude that miR-155 inhibits BMP signaling and growth inhibition in the lung epithelial cell line A549 and that inhibition of BMP functions may be relevant beyond EBV-infected B lymphocytes.

DISCUSSION

miR-155-mediated targeting of multiple members of the BMP signal transduction pathway. As the manuscript was in preparation, Rai et al. (31) similarly validated our earlier SMAD5 3′ UTR results (44) by showing that endogenous SMAD5 is inhibited by miR-155. Here, we show that miR-155 harbors the capacity to target multiple layers of the BMP signaling cascade. In addition to the central regulatory molecules, SMAD1 and SMAD5, miR-155 inhibits, at the RNA level, expression of cofactors that are required for high-affinity interactions between SMADs and responsive promoters. Although the role of HIVEP2 in mediating BMP responses in mammalian systems is at present limited, it has been established as a central regulator of BMP responses in *Drosophila* (3). We have also noted that the cofactor FOXO3, which plays a role in mediating SMAD2/3 binding to the p21 promoter in response to TGF-β (32, 36), contains predicted miR-155 target sites. We have thus far been unable to find reports demonstrating an interaction between members of the SMAD1/5/9 family with FOXO3. Nevertheless, given the relatedness of SMAD2/3 with SMAD1/5/9, this is a valid possibility. In such a case, FOXO3 will prove to be an additional cofactor in the BMP response pathway that is targeted by miR-155.

MYO10 is a downstream target of BMP signaling. Pi et al. (30) have shown in endothelial cells that BMP6 induces MYO10 expression, that MYO10 is localized to filopodia, and that it is required for filopodial assembly. Likewise, BMP6-dependent cellular alignment and directional migration require MYO10 (30). These data indicate a critical role for MYO10 in facilitating some of the phenotypic consequences of BMP6 signaling. Intriguingly, however, Pi et al. (30) found that MYO10 is also required for BMP6-dependent SMAD activation, indicating that in addition to its function in filopodial assembly, MYO10 participates in a requisite amplification loop for BMP signaling. This places MYO10 as an additional component in the BMP signaling cascade that is targeted by miR-155.

The targeting of multiple components of the BMP signaling cascade by miR-155 may be a mechanism for eliciting a strong influence on BMP signaling in the face of the intrinsic, moderate influences of microRNAs on an individual target gene. This strategy may also be a means of ensuring relatively strong inhibition in a wide array of tissues or cell types. The regulation of 3′ UTR structure (particularly length) appears to be an increasingly appreciated mechanism for modulating/dampening the influence of microRNA targeting (25, 34). In the face of cell-type-regulated alteration of 3′ UTR structure for individual miR-155 targets in the BMP pathway, an impact on overall signaling may remain relatively intact through the inhibition of other targets with long 3′ UTRs (which remain susceptible to miR-155 inhibition).

A notable omission in our study is SMAD9 which, like SMAD1 and SMAD5, facilitates core BMP signal transduction events from the cytoplasm to the nucleus. From a functional standpoint, it is important to note that the roles of SMAD1, SMAD5, and SMAD9 in transmitting BMP signaling appear to be largely redundant. The SMAD9 3′ UTR does not contain any significant seed complementarity to miR-155 (TargetScan [22]). It is reasonable to predict that if one member of this group is not susceptible to miR-155 targeting and is perhaps expressed at a slightly higher level than the other members of this family, transmission of cytoplasmic to nuclear signaling would be largely unaffected by miR-155. RNA-Seq analysis of the A549 transcriptome revealed that the level of SMAD9 mRNA in these cells is approximately 0.2 transcripts per cell, whereas the levels of SMAD1 and SMAD5 transcripts are approximately 6 and 11, respectively (see Fig. S2 in the supplemental material). Similar ratios were also found in Mutu I cells (G. Xu et al., submitted). The low abundance of SMAD9 transcripts (to a level that is well below 1 transcript per cell) likely means that cytoplasmic-to-nuclear transmission of BMP signaling is effectively mitigated by miR-155 in this cell system through targeting of only SMAD1 and SMAD5. Nevertheless, this arm of the BMP transduction pathway may be less affected

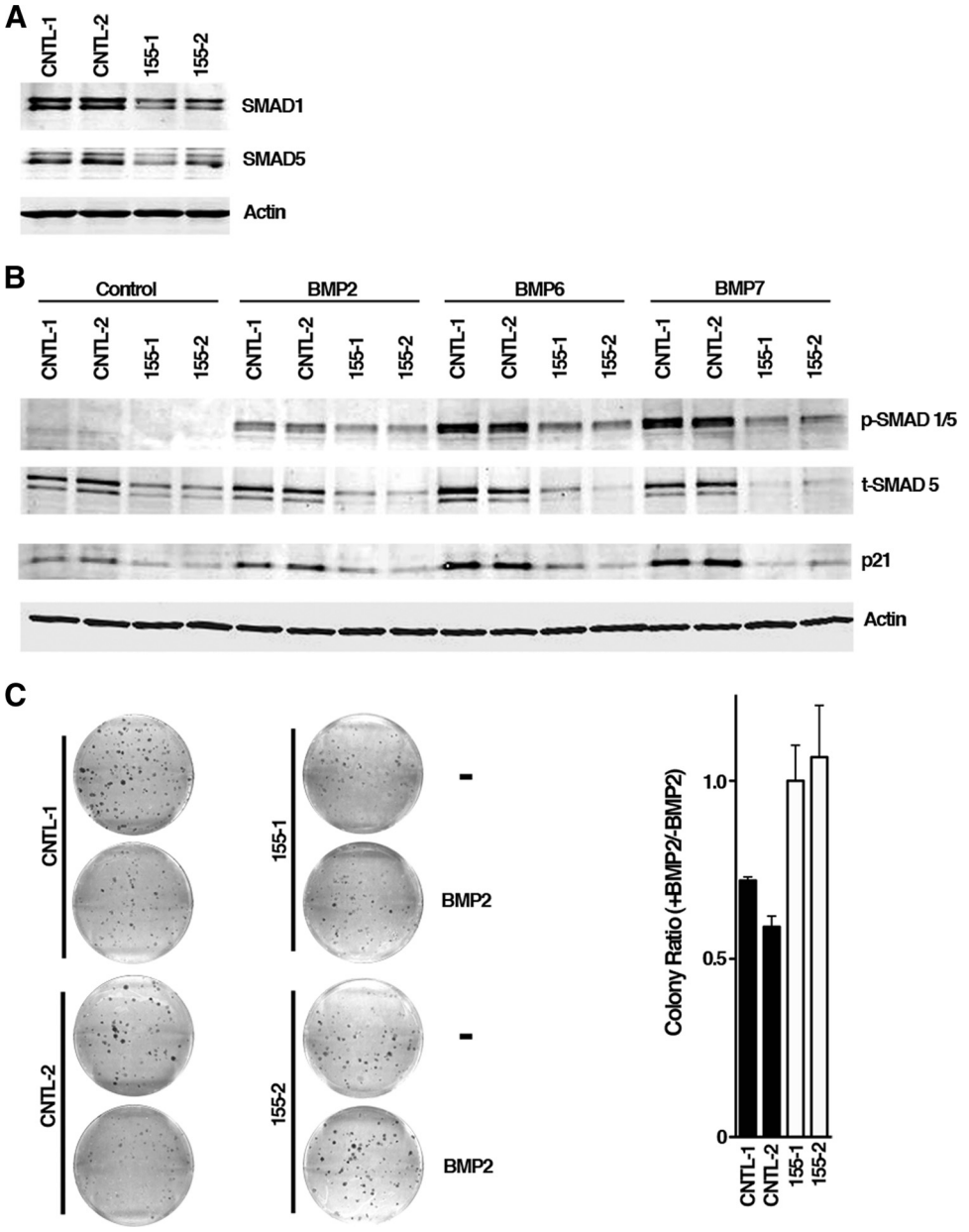

FIG. 6. miR-155 inhibits BMP signaling in the lung epithelial line, A549. (A) Western blot analysis of SMAD1 and SMAD5 expression was performed in A549 cells retrovirally transduced with control (CNTL-1 and CNTL-2) or miR-155 (155-1 and 155-2) retroviruses. (B) Control- or miR-155-transduced A549 cells were treated with the indicated BMP for 24 h and assessed for phospho-SMAD1/5 and the downstream target p21 by Western blot analysis (SMAD5 antibody is from Sigma). (C) Colony formation of retrovirally transduced A549 cells treated with BMP2 or untreated (−). The left panel shows a representative picture from one colony assay, and the right panel shows the calculated colony number ratios (with BMP/without BMP) for three repeats.

by miR-155 in cells where SMAD9 expression is more substantial. Cell-type-dependent alteration in polyadenylation site usage of other miR-155 targets in this pathway may similarly play a role in mitigating the overall response to miR-155 expression. Therefore, while miR-155 inhibits multiple components of the BMP signal transduction cascade and likely impedes BMP signaling in a range of settings, we still envision the possibility that, in certain physiological settings, a cell may be programmed to respond adequately to BMP signaling despite high levels of miR-155.

Role of miR-155 in suppressing BMP mediated signaling, virus reactivation, and antitumor effects. Type III latency has been demonstrated previously to actively suppress reactivation in tissue culture models (such as exposure to TGF-β and B-cell receptor activation) (10, 14, 26), and we have determined that, like Mutu III cells, two additional infected B-cell lines displaying type III latency are refractory to BMP-mediated reactivation (see Fig. S3 in the supplemental material). This property of type III latency may play a physiological role in enforcing latency during the natural infectious course of EBV. Patholog-

ically, the maintenance of a primarily latent state in EBV type III latency-associated malignancies likely contributes to the overall survival of the tumor since lytic replication typically has substantive negative influences on host cell survival.

In addition to EBV-associated malignancies, high levels of miR-155 are also observed in other lymphoid malignancies such as diffuse large B-dell lymphomas (DLBCL) (9, 21). A number of studies have now provided evidence that BMP signaling can inhibit B- and T-cell growth at various stages of lymphoid development (2, 6, 13, 18, 19, 37). Although it is likely that miR-155 contributes to oncogenesis at multiple levels, an ability to suppress BMP-mediated growth arrest signaling could be at least one contributing factor in tumor development/survival for some of these tumors. We have also shown here that miR-155 can inhibit BMP signaling, BMP-mediated induction of the cyclin-dependent kinase inhibitor p21, and BMP-mediated cell growth inhibition in a nonlymphoid setting (A549 cells). We expect that at least some nonlymphoid tumors exhibiting elevated levels of miR-155 may similarly enjoy increased survival characteristics in the face of negative influences of local BMPs.

Due to the functional overlap between cellular miR-155 and the Kaposi's sarcoma-associated herpesvirus (KSHV) (12, 38) and Marek's disease virus (MDV) (28) versions of miR-155, it is likely that these virus microRNAs will similarly influence these BMP signaling mediators. By analogy with EBV, they may influence the latency/lytic balance in these cells in response to BMP signaling, and/or they may promote cell proliferation/oncogenesis. The extent to which these virus homologues influence BMP signaling mediators and the impact of these interactions on virus biology will be borne out by future investigations.

ACKNOWLEDGMENTS

This work was supported by NIH grants (CA124311, CA130752, and CA138268) to Erik K. Flemington and an NIH COBRE (P20 RR020152) to P. Deininger.

We thank William Sugden and Ashok Aiyar for providing Mutu III cells.

REFERENCES

1. **Blanco Calvo, M., F. V. Bolos, V. V. Medina, G. G. Aparicio, P. S. Diaz, and P. E. Grande.** 2009. Biology of BMP signaling and cancer. Clin. Transl. Oncol. **11:**126–137.
2. **Bleul, C. C., and T. Boehm.** 2005. BMP signaling is required for normal thymus development. J. Immunol. **175:**5213–5221.
3. **Blitz, I. L., and K. W. Cho.** 2009. Finding partners: how BMPs select their targets. Dev. Dyn. **238:**1321–1331.
4. **Buckley, S., W. Shi, B. Driscoll, A. Ferrario, K. Anderson, and D. Warburton.** 2004. BMP4 signaling induces senescence and modulates the oncogenic phenotype of A549 lung adenocarcinoma cells. Am. J. Physiol. Lung Cell. Mol. Physiol. **286:**L81–L86.
5. **Cameron, J. E., C. Fewell, Q. Yin, J. McBride, X. Wang, Z. Lin, and E. K. Flemington.** 2008. Epstein-Barr virus growth/latency III program alters cellular microRNA expression. Virology **382:**257–266.
6. **Cejalvo, T., R. Sacedon, C. Hernandez-Lopez, B. Diez, C. Gutierrez-Frias, J. Valencia, A. G. Zapata, A. Varas, and A. Vicente.** 2007. Bone morphogenetic protein-2/4 signalling pathway components are expressed in the human thymus and inhibit early T-cell development. Immunology **121:**94–104.
7. **Clurman, B. E., and W. S. Hayward.** 1989. Multiple proto-oncogene activations in avian leukosis virus-induced lymphomas: evidence for stage-specific events. Mol. Cell. Biol. **9:**2657–2664.
8. **Dorsett, Y., K. M. McBride, M. Jankovic, A. Gazumyan, T. H. Thai, D. F. Robbiani, M. Di Virgilio, B. R. San-Martin, G. Heidkamp, T. A. Schwickert, T. Eisenreich, K. Rajewsky, and M. C. Nussenzweig.** 2008. MicroRNA-155 suppresses activation-induced cytidine deaminase-mediated Myc-Igh translocation. Immunity **28:**630–638.
9. **Eis, P. S., W. Tam, L. Sun, A. Chadburn, Z. Li, M. F. Gomez, E. Lund, and J. E. Dahlberg.** 2005. Accumulation of miR-155 and BIC RNA in human B cell lymphomas. Proc. Natl. Acad. Sci. U. S. A. **102:**3627–3632.
10. **Fukuda, M., W. Kurosaki, K. Yanagihara, H. Kuratsune, and T. Sairenji.** 2002. A mechanism in Epstein-Barr virus oncogenesis: inhibition of transforming growth factor-beta 1-mediated induction of MAPK/p21 by LMP1. Virology **302:**310–320.
11. **Ghosh-Choudhury, N., K. Woodruff, W. Qi, A. Celeste, S. L. Abboud, and G. Ghosh Choudhury.** 2000. Bone morphogenetic protein-2 blocks MDA MB 231 human breast cancer cell proliferation by inhibiting cyclin-dependent kinase-mediated retinoblastoma protein phosphorylation. Biochem. Biophys. Res. Commun. **272:**705–711.
12. **Gottwein, E., N. Mukherjee, C. Sachse, C. Frenzel, W. H. Majoros, J. T. Chi, R. Braich, M. Manoharan, J. Soutschek, U. Ohler, and B. R. Cullen.** 2007. A viral microRNA functions as an orthologue of cellular miR-155. Nature **450:**1096–1099.
13. **Hager-Theodorides, A. L., S. V. Outram, D. K. Shah, R. Sacedon, R. E. Shrimpton, A. Vicente, A. Varas, and T. Crompton.** 2002. Bone morphogenetic protein 2/4 signaling regulates early thymocyte differentiation. J. Immunol. **169:**5496–5504.
14. **Inman, G. J., and M. J. Allday.** 2000. Resistance to TGF-β1 correlates with a reduction of TGF-beta type II receptor expression in Burkitt's lymphoma and Epstein-Barr virus-transformed B lymphoblastoid cell lines. J. Gen. Virol. **81:**1567–1578.
15. **Iorio, M. V., and C. M. Croce.** 2009. MicroRNAs in cancer: small molecules with a huge impact. J. Clin. Oncol. **27:**5848–5856.
16. **Iorio, M. V., M. Ferracin, C. G. Liu, A. Veronese, R. Spizzo, S. Sabbioni, E. Magri, M. Pedriali, M. Fabbri, M. Campiglio, S. Menard, J. P. Palazzo, A. Rosenberg, P. Musiani, S. Volinia, I. Nenci, G. A. Calin, P. Querzoli, M. Negrini, and C. M. Croce.** 2005. MicroRNA gene expression deregulation in human breast cancer. Cancer Res. **65:**7065–7070.
17. **Jiang, J., E. J. Lee, and T. D. Schmittgen.** 2006. Increased expression of microRNA-155 in Epstein-Barr virus transformed lymphoblastoid cell lines. Genes Chromosomes Cancer **45:**103–106.
18. **Kersten, C., G. Dosen, J. H. Myklebust, E. A. Sivertsen, M. E. Hystad, E. B. Smeland, and E. Rian.** 2006. BMP-6 inhibits human bone marrow B lymphopoiesis—upregulation of Id1 and Id3. Exp. Hematol. **34:**72–81.
19. **Kersten, C., E. A. Sivertsen, M. E. Hystad, L. Forfang, E. B. Smeland, and J. H. Myklebust.** 2005. BMP-6 inhibits growth of mature human B cells; induction of Smad phosphorylation and upregulation of Id1. BMC Immunol. **6:**9.
20. **Kluiver, J., E. Haralambieva, D. de Jong, T. Blokzijl, S. Jacobs, B. J. Kroesen, S. Poppema, and A. van den Berg.** 2006. Lack of BIC and microRNA miR-155 expression in primary cases of Burkitt lymphoma. Genes Chromosomes Cancer **45:**147–153.
21. **Kluiver, J., S. Poppema, D. de Jong, T. Blokzijl, G. Harms, S. Jacobs, B. J. Kroesen, and A. van den Berg.** 2005. BIC and miR-155 are highly expressed in Hodgkin, primary mediastinal and diffuse large B cell lymphomas. J. Pathol. **207:**243–249.
22. **Lewis, B. P., C. B. Burge, and D. P. Bartel.** 2005. Conserved seed pairing, often flanked by adenosines, indicates that thousands of human genes are microRNA targets. Cell **120:**15–20.
23. **Lu, F., A. Weidmer, C. G. Liu, S. Volinia, C. M. Croce, and P. M. Lieberman.** 2008. Epstein-Barr virus-induced miR-155 attenuates NF-κB signaling and stabilizes latent virus persistence. J. Virol. **82:**10436–10443.
24. **Lu, J., G. Getz, E. A. Miska, E. Alvarez-Saavedra, J. Lamb, D. Peck, A. Sweet-Cordero, B. L. Ebert, R. H. Mak, A. A. Ferrando, J. R. Downing, T. Jacks, H. R. Horvitz, and T. R. Golub.** 2005. MicroRNA expression profiles classify human cancers. Nature **435:**834–838.
25. **Mayr, C., and D. P. Bartel.** 2009. Widespread shortening of 3′UTRs by alternative cleavage and polyadenylation activates oncogenes in cancer cells. Cell **138:**673–684.
26. **Miller, C. L., J. H. Lee, E. Kieff, and R. Longnecker.** 1994. An integral membrane protein (LMP2) blocks reactivation of Epstein-Barr virus from latency following surface immunoglobulin crosslinking. Proc. Natl. Acad. Sci. U. S. A. **91:**772–776.
27. **Miyazono, K., S. Maeda, and T. Imamura.** 2005. BMP receptor signaling: transcriptional targets, regulation of signals, and signaling cross-talk. Cytokine Growth Factor Rev. **16:**251–263.
28. **Morgan, R., A. Anderson, E. Bernberg, S. Kamboj, E. Huang, G. Lagasse, G. Isaacs, M. Parcells, B. C. Meyers, P. J. Green, and J. Burnside.** 2008. Sequence conservation and differential expression of Marek's disease virus microRNAs. J. Virol. **82:**12213–12220.
29. **Motsch, N., T. Pfuhl, J. Mrazek, S. Barth, and F. A. Grasser.** 2007. Epstein-Barr virus-encoded latent membrane protein 1 (LMP1) induces the expression of the cellular microRNA miR-146a. RNA Biol. **4:**131–137.
30. **Pi, X., R. Ren, R. Kelley, C. Zhang, M. Moser, A. B. Bohil, M. Divito, R. E. Cheney, and C. Patterson.** 2007. Sequential roles for myosin-X in BMP6-dependent filopodial extension, migration, and activation of BMP receptors. J. Cell Biol. **179:**1569–1582.
31. **Rai, D., S. W. Kim, M. R. McKeller, P. L. Dahia, and R. C. Aguiar.** 2010. Targeting of SMAD5 links microRNA-155 to the TGF-beta pathway and lymphomagenesis. Proc. Natl. Acad. Sci. U. S. A. **107:**3111–3116.
32. **Reynisdottir, I., K. Polyak, A. Iavarone, and J. Massague.** 1995. Kip/Cip and

Ink4 Cdk inhibitors cooperate to induce cell cycle arrest in response to TGF-beta. Genes Dev. **9:**1831–1845.

33. **Rodriguez, A., E. Vigorito, S. Clare, M. V. Warren, P. Couttet, D. R. Soond, S. van Dongen, R. J. Grocock, P. P. Das, E. A. Miska, D. Vetrie, K. Okkenhaug, A. J. Enright, G. Dougan, M. Turner, and A. Bradley.** 2007. Requirement of bic/microRNA-155 for normal immune function. Science **316:**608–611.
34. **Sandberg, R., J. R. Neilson, A. Sarma, P. A. Sharp, and C. B. Burge.** 2008. Proliferating cells express mRNAs with shortened 3′ untranslated regions and fewer microRNA target sites. Science **320:**1643–1647.
35. **Schuster, C., S. Chasserot-Golaz, and G. Beck.** 1991. Activation of Epstein-Barr virus promoters by a growth-factor and a glucocorticoid. FEBS Lett. **284:**82–86.
36. **Seoane, J., H. V. Le, L. Shen, S. A. Anderson, and J. Massague.** 2004. Integration of Smad and forkhead pathways in the control of neuroepithelial and glioblastoma cell proliferation. Cell **117:**211–223.
37. **Sivertsen, E. A., K. Huse, M. E. Hystad, C. Kersten, E. B. Smeland, and J. H. Myklebust.** 2007. Inhibitory effects and target genes of bone morphogenetic protein 6 in Jurkat TAg cells. Eur. J. Immunol. **37:**2937–2948.
38. **Skalsky, R. L., M. A. Samols, K. B. Plaisance, I. W. Boss, A. Riva, M. C. Lopez, H. V. Baker, and R. Renne.** 2007. Kaposi's sarcoma-associated herpesvirus encodes an ortholog of miR-155. J. Virol. **81:**12836–12845.
39. **Tam, W., D. Ben-Yehuda, and W. S. Hayward.** 1997. bic, a novel gene activated by proviral insertions in avian leukosis virus-induced lymphomas, is likely to function through its noncoding RNA. Mol. Cell. Biol. **17:**1490–1502.
40. **Teng, G., P. Hakimpour, P. Landgraf, A. Rice, T. Tuschl, R. Casellas, and F. N. Papavasiliou.** 2008. MicroRNA-155 is a negative regulator of activation-induced cytidine deaminase. Immunity **28:**621–629.
41. **Thai, T. H., D. P. Calado, S. Casola, K. M. Ansel, C. Xiao, Y. Xue, A. Murphy, D. Frendewey, D. Valenzuela, J. L. Kutok, M. Schmidt-Supprian, N. Rajewsky, G. Yancopoulos, A. Rao, and K. Rajewsky.** 2007. Regulation of the germinal center response by microRNA-155. Science **316:**604–608.
42. **Volinia, S., G. A. Calin, C. G. Liu, S. Ambs, A. Cimmino, F. Petrocca, R. Visone, M. Iorio, C. Roldo, M. Ferracin, R. L. Prueitt, N. Yanaihara, G. Lanza, A. Scarpa, A. Vecchione, M. Negrini, C. C. Harris, and C. M. Croce.** 2006. A microRNA expression signature of human solid tumors defines cancer gene targets. Proc. Natl. Acad. Sci. U. S. A. **103:**2257–2261.
43. **Yanaihara, N., N. Caplen, E. Bowman, M. Seike, K. Kumamoto, M. Yi, R. M. Stephens, A. Okamoto, J. Yokota, T. Tanaka, G. A. Calin, C. G. Liu, C. M. Croce, and C. C. Harris.** 2006. Unique microRNA molecular profiles in lung cancer diagnosis and prognosis. Cancer Cell **9:**189–198.
44. **Yin, Q., J. McBride, C. Fewell, M. Lacey, X. Wang, Z. Lin, J. Cameron, and E. K. Flemington.** 2008. MicroRNA-155 is an Epstein-Barr virus-induced gene that modulates Epstein-Barr virus-regulated gene expression pathways. J. Virol. **82:**5295–5306.